Original Article

DEVELOPMENT, FORMULATION, AND EVALUATION OF SODIUM ALGINATE-G-POLY (ACRYL AMIDE-CO-ACRYLIC ACID/CLOISTE-30B)/AGNPs HYDROGEL COMPOSITES AND THEIR APPLICATIONS IN PACLITAXEL DRUG DELIVERY AND ANTICANCER ACTIVITY

B. H. NANJUNDA REDDY[1,2], PRADIPTA RANJAN RAUTA[3], V. VENKATA LAKSHMI[4*], SWAMY SREENIVASA[2]

[1]Department of Chemistry, Amrita School of Engineering, Bengaluru, Amrita Vishwa Vidyapeetham, India, [2]Department of Studies and Research in Chemistry, Tumkur University, Tumkur, India, [3]NIT Rourkela, Rourkela, Odisha, India, [3, 4]Department of Chemistry, AMC Engineering College, Bannerghatta Road, Bengaluru, India
Email: *laxmimurthy@rediffmail.com

ABSTRACT

Objective: The objective of this study was to develop, formulate and evaluate the sodium alginate grafted poly (acrylamide-co-acrylic acid/cloisite-30B/silver nanoparticle hydrogel composites (SA-PAAm-PAAc/C30B/AgNPs) with varying weight percentage (wt %) of cloisite-30B clay for paclitaxel targeted delivery and anticancer activity.

Methods: Polymer hydrogel composites of different wt % of cloisite-30B modified clay dispersed sodium alginate (SA) grafted polyacrylamide-co-polyacrylic acid were prepared via in situ free radical initiation polymerization reaction technique. *In vitro* release of paclitaxel (PT) anticancer drug and anticancer studies were performed. The formulations were further evaluated for swelling, drug encapsulation, drug delivery, anticancer activity study, Fourier transforms infrared spectroscopy (FT-IR), thermogravimetric (TGA), differential scanning calorimeter (DSC) and x-ray diffraction (XRD) characterizations.

Results: FT-IR spectroscopy of various composite hydrogel formulations displayed good compatibility between sodium alginate, polyacrylamide, and polyacrylic acid polymers. The thermal study reveals that the formulations with clay (C30B) and AgNPs in hydrogel composites exhibit good thermal stability and less % of weight loss (wt. loss) compared to pure formulations. Further, the highest encapsulation efficiency was shown by the formulation S_{0-0+D} (72.66±5.92%) and least encapsulation efficiency was shown by S_{75Ag+D} (41.33±3.12%) compared to rest of the formulations and S_{50Ag+D} and S_{75Ag+D} samples exhibits relatively slightly higher and sustained cumulative release rate of PT drug at an average rate of 80±9 % within 72 h and also shows relatively better anticancer activity compared to other formulations.

Conclusion: Formulations S_{50Ag+D} and S_{75Ag+D} were found to be best formulations with a higher cumulative percentage of PT drug release and showed better anticancer activity

Keywords: Sodium alginate, Cloisite-30B, AgNPs, Hydrogel, Paclitaxel, Drug delivery, anticancer, Acrylamide

INTRODUCTION

The biomaterials research field has broadened in the last three to four decades including drug release systems, anticancer examine, immunological kits, biosensors and plenty of other biomedical applications [1]. Polymer-clay nanocomposites are a class of hybrid biomaterial substances composed of natural polymer matrices and nanoscale organophilic clay fillers which include cloisite-30B which is methyl, tallow, bis-2 hydroxyethyl quaternary ammonium, where tallow is 65% C18, 30% C16, and 5% C14. Clay minerals are widely used substances in drug products as delivery vehicles [2]. Montmorillonite (MMT) can offer the mucoadhesive capability for the nanoparticle to cross the gastrointestinal (GI) barrier. MMT is likewise a robust detoxifier, which belongs to the structural family of 2:1 phyllosilicate. MMT could absorb nutritional toxins, pathogenic bacteria related gastrointestinal route, H+ions in acidosis and metabolic toxins including steroidal metabolites associated with pregnancy. Hence blending chitosan with cloisite-30B (MMT) can enhance the drug releasing and anticancer property of the composite hydrogels [3, 4].

New technologies depend upon the improvement of recent materials, and these might also surely be the aggregate of recognized additives. The structural combination of a polymer hydrogel network with a nanoparticles (metals, non-metals, metallic oxides, and polymeric moieties) holds the promise of presenting advanced capability to the composite material with applications in diverse fields, such as catalysis, electronics, bio-sensing, drug delivery, nano-medicine, antibacterial interest and environmental remediation [5].

The sodium alginate hydrogels are in large part used because of their high biocompatibility. During the last decade, a huge part of the investigation in the biomedical discipline has resolved many problems of drug delivery vehicles and bioactive macromolecules. Lately, the application of alginate hydrogels as scaffolding materials has attracted the attention in the field of tissue engineering, wound dressing, drug delivery and some other biomedical uses. A lot of reports have recommended that some alginate dressings can enhance wound recuperation by stimulating monocytes to provide high levels of cytokines which include interleukin-6 and tumor necrosis factor-α [6]. Formation of these pro-inflammatory cytokines inside the wounded tissue is vital for tissue repair mechanisms that in the end result in wound healing [7]. Due to this, alginates are frequently used as they relatively ease with which they could undergo gelation with divalent cations under suitable conditions which are appropriate for bio macromolecules and living cells.

Synthetically varied methods were proposed for the development of AgNPs and AgNP-composites by means of incorporating metal ions into thin films of titania, sol-gels, polyelectrolyte multilayer films, porous polymers, AgNPs doped natural polymers and viscous resins loaded with AgNPs, which are noticeably appropriate for biomedical applications and drug delivery [8]. In particular, nanosilver (AgNPs) based wound dressings have acquired the appreciation for scientific applications, however; dermal toxicity is reported [9-11]. Therefore, the mixture of a gel system with silver nanoparticles and cloisite-30B will be a higher desire for the drug delivery and anticancer activity in the form as such. 3-dimensional (3D) gel (nano, micro, and hydrogel) networks are quite suitable for the in situ synthesis of silver nanoparticles (AgNps) than the maximum of the traditional non-aqueous or polymer related synthetic processes [8].

Paclitaxel (PT) is one of the best wide-spectrum of chemotherapeutic marketers in the treatment of the extensive variety of cancers, together

with lung, ovarian, and breast cancers. But, its scientific application has been restricted due to its poor water solubility. Due to its low water solubility, paclitaxel is formulated in an aggregate of cremophor EL and dehydrated ethanol (50:50, v/v) a combination called taxol. However, taxol has some severe side consequences related to cremophor EL and ethanol. Its contemporary medical management uses the adjuvant of great facet outcomes and has undesired pharmacokinetics and bio distribution. there is, hence, a need for the development of exchange drug transport systems of PT to enhance its solubility, permeability and balance and further to promote a sustained, controlled and targeted delivery in order to increase its therapeutic results and decrease its surface properties [12].

The aim of this work was to develop a novel drug delivery system based on composite gel formation technique and which can be commercially exploited for the well-being of the society [13]. Further, the effective incorporation of nanosilver particles into the polymer clay hydrogel composites network and these hydrogel composites are efficiently utilized for *in vitro* paclitaxel (PT) drug delivery and anticancer activity.

MATERIALS AND METHODS

Materials

Sodium alginate (SA), acryl amide (AAm), acrylic acid (AAc), cloisite-30B (C30B) nanoclay N,N'-methylene bis acryl amide (MBA), as cross linking agent, N,N,N',N-tetramethyl ethylene diamine (TEMED) as an accelerator, ammonium persulphate (APS) as an initiator, silver nitrate ($AgNO_3$) as precursor, sodium borohydride ($NaBH_4$) as reducing agent, paclitaxel (PT), as an anticancer drug (a gift sample from my research friend working for Thrombosis Cancer Research Center, (TCRC) Bangalore, India) etc. obtained from Sigma Aldrich Bangalore, India. The chemicals were used as it received without any further purification and double distilled water (DDW) was used throughout this experiment

Development of sodium alginate-poly (acrylamide-co-acrylic acid/closite-30B) hydrogel composites

Sodium alginate poly (acryl amide-co-acrylic acid/closite-30B)/ silver nano particle (SA-PAAm-PAAc/C30B/AgNPs) composite

hydrogel are obtained by preparing sodium alginate solution, by dissolving 0.15 gm SA in 5 ml (3% wt/vol. ratio wrt polymer) of double distilled water in a 100 ml beaker and stirred using magnetic stirrer about 30 min., and for this solution 2 ml of each of monomers, acryl amide, and acrylic acid solutions were added (1 gm in 2 ml distilled water),further100 mg of MBA (100 mg in 5 ml distilled water), 500 mg of APS (500 mg in 5 ml of distilled water), 20 mg of TEMED (20 mg in 5 ml of distilled water) solutions were added to the above SA solution and mixed thoroughly using magnetic stirrer (30 min.), for this solution, different weight percentages of MMT clay (cloisite-30B nanoclay) were mixed (previously ultrasonicated for one hour each wt. % of cloisite-30B nano clay in 15 ml of DDW) and finally the respective solutions are kept in air tight capped test tube like bottles and kept in hot water bath by maintaining the temperature of about 70-80 °C results in the free radical polymerization reaction and after completion of the reaction, the respective polymer hydrogel composites are formed which are further carefully cut into desired shapes and allowed to stay in double distilled (DDW) for about 3 d in a container to remove all the un-reacted components or excess chemicals. Further, these samples were oven dried for 12 h at ambient temperature and will be used for the synthesis of silver nanoparticles, swelling studies, drug delivery studies anticancer activity and other characterizations.

Development of SA-g-poly (acrylamide-co-acrylic acid/cloisite 30B/AgNPs hydrogel composites

SA-PAAm-PAAc/C30B/AgNPs based hydrogel composites had been prepared by incorporating dry hydrogel disks into the double distilled water and equilibrated for 4 d. Those gels have been transferred to brown shade airtight bottles containing 50 ml of aqueous AgNO3 and which is allowed equilibrating for a day. This allows the transfer of silver ions from the solution into the hydrogel networks through ion exchange process. The silver ions in SA-PAAm-PAAc/C30B/AgNPs hydrogel composites had been reduced through NaBH4 reducing agent within 2 h into silver nanoparticles in the network of hydrogel composites. The developed SA-PAAm-PAAc/C30B/AgNPs hydrogel composites have been named as S_{0-0}, S_{50-0}, S_{0-Ag}, S_{25-Ag}, S_{50-Ag}, and S_{75-Ag} and the scheme of reaction variables are tabulated in table 1.

Table 1: Composition of SA-g-Poly (acrylamide-co-acrylic acid)/C30B/Ag hydrogel composites

S. No.	Sample code	Polymer (SA) 10 ml	Monomer (AAm) 5 ml	Monomer (AAc) 5 ml	Clay (C30B) 15 ml	Crosslinker (MBA) 5 ml	Accelerator (TEMED) 5 ml	Initiator (APS) 5 ml	NPs (Ag)
1	S0-0	300 mg/10 ml	1g/5 ml	1g/5 ml	0%	100 mg/5 ml	20 mg/5 ml	500 mg/5 ml	Nil
2	S0-Ag	300 mg/10 ml	1g/5m[l	1g/5 ml	0%	100 mg/5 ml	20 mg/5 ml	500 mg/5 ml	Ag
3	S25-Ag	300 mg/10 ml	1g/5 ml	1g/5 ml	25% (75 mg)	100 mg/5 ml	20 mg/5 ml	500 mg/5 ml	Ag
4	S50-0	300 mg/10 ml	1g/5 ml	1g/5 ml	50% (150 mg)	100 mg/5 ml	20 mg/5 ml	500 mg/5 ml	Nil
5	S50-Ag	300 mg/10 ml	1g/5 ml	1g/5 ml	50% (150 mg)	100 mg/5 ml	20 mg/5 ml	500 mg/5 ml	Ag
6	S75-Ag	300 mg/10 ml	1g/5 ml	1g/5 ml	75% (225 mg)	100 mg/5 ml	20 mg/5 ml	500 mg/5 ml	Ag

[SA: Sodium alginate; AAM: Acrylamide; AA: Acrylic acid; C30B: cloisite-30B; MBA: N,N'-methylenebisacrylamide; TEMED: N,N,N',N' Tetramethylethylenediamine; APS: Ammonium per sulfate; Ag NPs: Ag nanoparticles]

Swelling studies

The percentage of swelling fraction (% SF) and the percentage of equilibrium swelling (% ES) have been calculated as shown in the equations 1 and 2

$$\% \text{ Swelling fraction [SF]} = Ws/Wd \ldots\ldots\ldots\ldots (1)$$

$$\% \text{ Equilibrium swelling [Q]} = \frac{Ws}{Wd} \times 100 \ldots\ldots\ldots (2)$$

Where Ws and Wd are mass of swollen SA-PAAm-PAAc/C30B/AgNPs hydrogel composites for a given time t and dried hydrogel composites.

Here, Q is the equilibrium mass of swollen SA-PAAm-PAAc/ C30B/AgNPs hydrogel composites. Equilibrium swelling experiments on SAPAC30B/AgNPs hydrogel composites have been carried out in double distilled water (DDW) at 30 °C (±05 °C).

Encapsulation efficiency of SA-PAAm-PAAc/C30B/AgNPs hydrogel composites

Paclitaxel becomes encapsulated into SA-PAAm-PAAc/C30B/AgNPs hydrogel composites via a swelling equilibrium method. The hydrogels disks were immersed in the known concentration of drug solution and allowed them to swell for 24 h at 37 °C. The solubility of paclitaxel in double distilled water is 13 mg/ml, which is appreciably is quite low. However, sodium salts can increase the solubility of paclitaxel up to 65 mg/ml. in order to load the high amount of drug content into the polymeric network, the gel disks have been immersed in a sodium salt of paclitaxel aqueous solution. Equilibration technique allows the absorption of paclitaxel by the SA-PAAm-PAAc/C30B/AgNPs hydrogel composites and the drug-loaded formulations are named asS_{0-0+D}, S_{50-0+D}, S_{0-Ag+D}, $S_{25-Ag+D}$, $S_{50-Ag+D}$, and $S_{75-Ag+D}$. The loading efficiency of paclitaxel in the SA-PAAm-PAAc/C30B/AgNPs hydrogel composites were measured using uv-

visible spectrophotometer (UV-3092, LAB INDIA, India). Paclitaxel-loaded hydrogel composites were placed in 50 ml of buffer medium (pH=7) and stirred vigorously for 48 h to extract paclitaxel from the hydrogel composites. The solution became filtered and analyzed by means of the uv-visible spectrophotometer at a particular wavelength (λ max. =230 nm). Percentage of paclitaxel loading and the encapsulation efficiency (EE) of SA-PAAm-PAAc/C30B/AgNPs hydrogel composites had been calculated with the aid of the subsequent equations 3 and 4, and the ensuing statistics were compiled in table2.

$$\% \text{ of Drug loading } [D] = \frac{\text{Weight of the drug adding (g)}}{\text{weight of the polymer+Drug}} \times 100 \ldots\ldots\ldots (3)$$

$$\% \text{ Encapsulation efficiency } [ES] = \frac{\text{Total amount of drug(g)}}{\text{the actual amount of drug}} \times 100. (4)$$

In vitro drug release studies

In vitro, drug release experiments have completed the usage of the dissolution system (DS8000, LABINDIA, India) attached with 8 baskets. Drug release rates have been measured at 37 °C below a 100rpm velocity. Drug release kinetics was analyzed by plotting the % cumulative release (Mt/M∞) v/s time (t). The SA-PAAm-PAAc/C30B/AgNPs hydrogel composites had been studied in the buffer medium at pH=7.2 and pH=2, at the temperatures of 25 °C and 37 °C for distinctive formulations.

FT-IR characterizations

Fourier transformation infrared (FT-IR) spectroscopy analysis performed to corroborate the possibility of interaction between the clay, AgNPs, drug and the polymer. % of transmittance of FT-IR spectrum vs wave number was measured using Bruker ALPHA Spectrophotometer (Ettlinger, Germany) with a resolution of 4 cm⁻¹ and scanned between the range 4000 and 500 cm⁻¹.

DSC-TGA studies

The thermal stability and thermal degradation of formulated hydrogels had been characterized by using differential scanning calorimetry (DSC) and thermogravimetric (TGA) evaluation (Netzch DSC 200 Fs). The samples (~12 mg) were sealed in aluminium pans and heated underneath nitrogen by using heating rate of 100 °C/min., the heat flow being recorded from 300 °C to 800 °C. Indium was used as reference material to calibrate the temperature and energy scales of the DSC system.

XRD analysis

The X-ray powder diffraction (XRD) patterns of prepared hydrogels were obtained using X-ray diffractometer (RigakuUltima IV, Japan) equipped with Ni filter and Cu Kα (l = 1.54056 Å) radiation source.

Cytocompatibility assessment through MTT assay study

The biocompatibility of the prepared SA-PAAm-PAAc/C30B/AgNPshydrogel composite gels has been determined by the following popular protocol with mild modifications [14]. In short, HaCaT cells and MCF-7 (breast cancer mobile strains) cells were procured from NCCS, Pune, India, and the cells have been grown in DMEM medium. After 80% confluency, the cells had been trypsinized and 3000 cells properly have been seeded in 96 well plates and stored in a CO₂ incubator at 37 °C. Meantime, the hydrogels have been cut into small pieces (1x1 cm) and stored in a dialysis bag and both the ends were sealed. The dialysis bag was immersed in 20 ml of PBS solution and become stored in constant stirring at 100 rpm for 24 h. The leachets from the hydrated hydrogels have been diluted serially with the DMEM media (0%, 12.5%, 25%, 50%, and 100%) and then 200 ml of extract and the diluted solution added in a 96-well plate. For the control, 100% media had been used to evaluate most of the dilution. The addition of leachets the 96 well plates were sooner or later stored in a CO₂ incubator at 37 °C. To detect the cell viability MTT experimental solution prepared from a stock solution of 5 mg/ml in growth medium without FBS to the final concentration of 0.8 mg/ml, 100 µl of MTT solution become delivered and incubated for 4 h. After 4 h of incubation, the MTT solution was discarded, and 100 µl of DMSO solvent discharged in every well under dark, followed by an incubation of 15 min. and the optical density (OD) of the formazan product was read at 595 nm in a microplate reader (Perkin Elmer, Waltham, MS, USA).

Statistical analysis

All the experiments were done in triplicate, and the results were expressed in terms of mean±SD and were analyzed statistically by one-way analysis of variance [ANOVA] at the level of significance

RESULTS AND DISCUSSION

Swelling studies

It is the measurement of swelling property of swellable hydrogel polymer composites. The study is done by immersing equal weights of dried hydrogel samples in distilled water at 25 °C for 3 d and determinin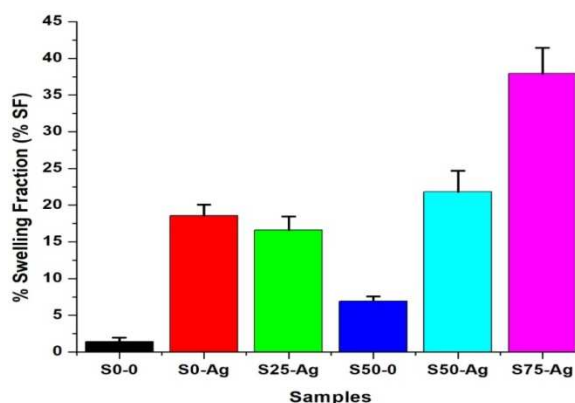g the swelling fraction using the equation (Eqn.-5) [15]. The fig. 1 indicates the swelling property of cloisite-30B clay supported silver nanoparticles-sodium alginate-g-polyacrylamide/acrylic acid/hydrogel composites (SA-PAAm-PAAc/C30B/AgNPs). The graph is plotted as % of weight gained (%W g/g) v/s various samples such as S_{0-0}, S_{0-Ag}, S_{25-Ag}, S_{50-0}, S_{50-Ag}, and S_{75-Ag}. Swollen hydrogels had been treated first with the $AgNO_3$ solution and then with the $NaBH_4$ solution as explained in the experimental section.

The equilibrium swelling ratio (Q) is calculated from the equation: [Q] =We/Wd ………(5)

In which we are the weight of water within the swollen hydrogel and Wd is the dry weight of the hydrogel.

Fig. 1: Indicates the swelling property of Cloisite-30B clay supported silver nanoparticles-Sodium alginate-g-poly Acrylamide/acrylic acid hydrogel composites. The graph is plotted as % of weight gained (%Wt g/g) versus various samples such as S_{0-0}, S_{0-Ag}, S_{25-Ag}, S_{50-0}, S_{50-Ag}, and S_{75-Ag}. The results were expressed as the mean of three observation, mean±SD (n =3)

The swelling ability of the anticancer and carriers for the improvement of site-specific delivery of drugs and inorganic substances like clay (C30B), AgNPs in composite hydrogels play a critical role in the antibacterial interest, anticancer activity, wound restoration system, and other biomedical applications. Fig. 1 illustrates the swelling ability of the S_{0-0}, S_{0-Ag}, S_{25-Ag}, S_{50-0}, S_{50-Ag}, and S_{75-Ag} with time t. The order of the swelling capability of hydrogels follows $S_{75-Ag}>S_{50-Ag}>S_{25-Ag}>S_{0-Ag}>S5_{0-0}>S_{0-0}$ The S_{0-Ag}, S_{25-Ag} and S_{50-Ag} hydrogel composites show the moderate swelling ratio (22 g/g) than the S_{75-Ag} hydrogel (37g/g). Lower swelling capacity was shown by the samples S_{0-0} and S_{50-0} hydrogel composites may be attributed to the absence of AgNPs in the SA/AAm/AAc monomers reduces the pore sizes in the hydrogels and presence of cloisite-30B may be accountable to provide the extra cross-links inside the chain networks. The higher crosslinks restrict the water penetration for swelling. Apparently, the porous S_{75-Ag} hydrogel composite show higher swelling ability due to presence cloisite-30B in combination with Ag NPs increases the porosity in their network structures because of intermolecular interaction between water molecules in clay galleries and the lone pair electrons of–NH₂ and–OH groups

present in SA-PAAm-PAAc chains. Interestingly this pattern of swelling is also reasonable for the presence of AgNPs in nanocomposite hydrogels due to the fact once the Ag nanoparticles (AgNPs) are shaped in the gel networks; the general porosity of the system will increase allowing an extra number of water molecules inside the gel [16]. One extra reason for this behavior is that the formed nanoparticles (AgNPs) have distinctive sizes with different charge surfaces within the gel networks causing absolute enlargement of the networks and in addition the presence of greater hydrophilic groups of modified clay (C30B) in conjunction with AgNPs that allow a large amount of water to get into the hydrogel. As the clay content increases, in the presence of AgNPs in the hydrogel composites results in slightly improved swelling capacity.

Encapsulation efficiency of paclitaxel drug

Hydrogels had been loaded with paclitaxel, an anticancer drug by means of swelling equilibrium method. The hydrogels have been allowed to swelling in the paclitaxel solution of recognized concentration for 24 h at 37 °C. In general solubility of paclitaxel in water may be very less (13 mg/ml), but the solubility of paclitaxel increases up to 5 mg/ml. in DMSO that allows loading the most paclitaxel into the hydrogel matrix, hydrogel disks were immersed in aqueous solution; paclitaxel, so the drug solvent become absorbed onto the SA-PAAm-PAAc/C30B/AgNPs composite hydrogels. The loading performance of paclitaxel in the hydrogel was determined by spectrophotometrically. Approximately 0.53 gm of the drug-loaded hydrogel was placed in 50 ml of buffer solution and stirred vigorously for 48 h to extract the drug from the hydrogels, the solution becomes filtered and assayed by UV spectrophotometer (LAB INDIA, UV-3092) at constant λ max. = 230 nm. The results of % paclitaxel loading and encapsulation efficiency have been calculated and listed, and as shown in table 2, in which it depends on the polymer type and physical nature of the drug (either in solid form or in solution form) during processing.

Table 2: Encapsulation efficiency (%) of paclitaxel drug

S. No.	Code	Encapsulation efficiency (%)
1	S_{0-0+D}	72.66±5.92
2	S_{0-Ag+D}	56.34±3.95
3	$S_{25-Ag+D}$	51.44±4.56
4	S_{50-0+D}	64.67±4.92
5	$S_{50-Ag+D}$	49.67±2.57
6	$S_{75-Ag+D}$	41.33±3.12

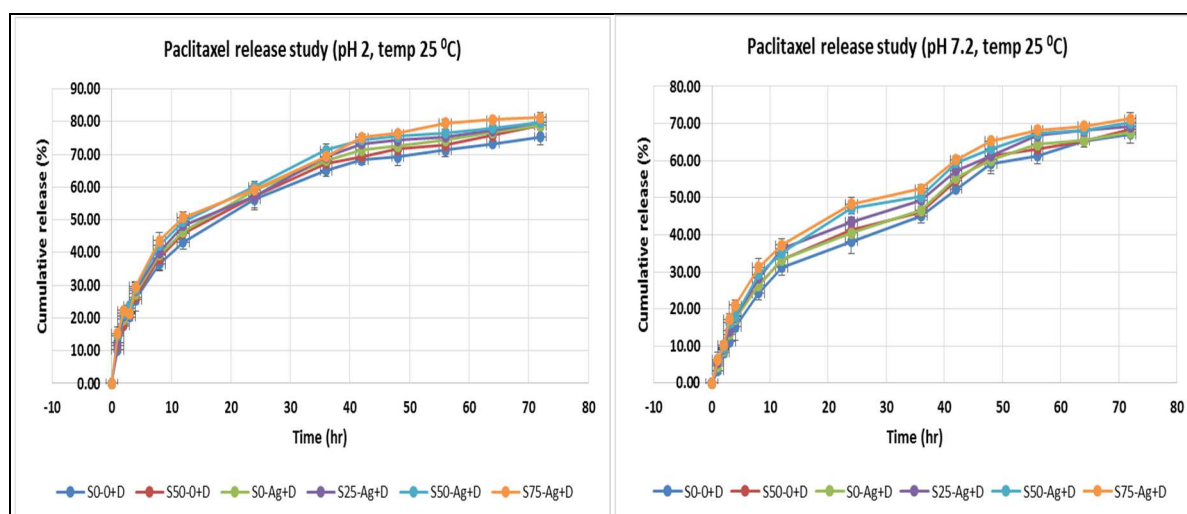Data were expressed as the mean of three observation, mean±SD (n=3).

The loading efficiencies had been reduced with the presence of clay in addition to AgNPs. In case of S_{0-0+D}, the drug encapsulation efficiency was 72.66±5.92%. Due to the presence of AgNPs in S_{0-Ag+D}; the encapsulation efficiency was decreased to 56.34±3.95%. Similarly, due to the presence of clay in S_{50-0+D} (50% clay), the encapsulation efficiency was slightly increased to 64.67±4.92%. In other samples ($S_{25-Ag+D}$, $S_{50-Ag+D}$, $S_{75-Ag+D}$), the encapsulation efficiencies were decreased from 51.44±4.56 to 41.33±3.12% due to increase in the concentration of clay. The decreasing tendency may be attributed to the crosslinking nature of clay (closite-30B). Indeed, closite-30B acts as cross-linking points in the network, which is responsible for the increase of crosslinking density of hydrogel network as the increase of clay content. The more is cross-linking density, the worse the elasticity of the polymer chains [17] which can limit the penetration of paclitaxel into hydrogel network, results in a decrease of loading capacity of the drug. Similar outcomes were additionally observed [18] in the case of chitosan-g-poly (acrylic acid) loaded theophylline hydrogels [18]. Additionally, the excess clay acts as the filler and prevents paclitaxel enter into the polymeric network which is likewise accountable for the decrease of encapsulation efficiency (EE).

In vitro release of paclitaxel from SA-PA hydrogel composites have been evaluated in the medium of simulated gastrointestinal fluids (buffer medium of pH 2 and 7.2)

***In vitro* drug release study**

In vitro release studies of paclitaxel from SA-PAAm-PAAc/C30B/AgNPs hydrogel composites have been evaluated for the stimulated gastro-intestinal fluids (SGF) and the graphs have been plotted by plotting percentage of cumulative release versus time in hours as shown in fig. 2.
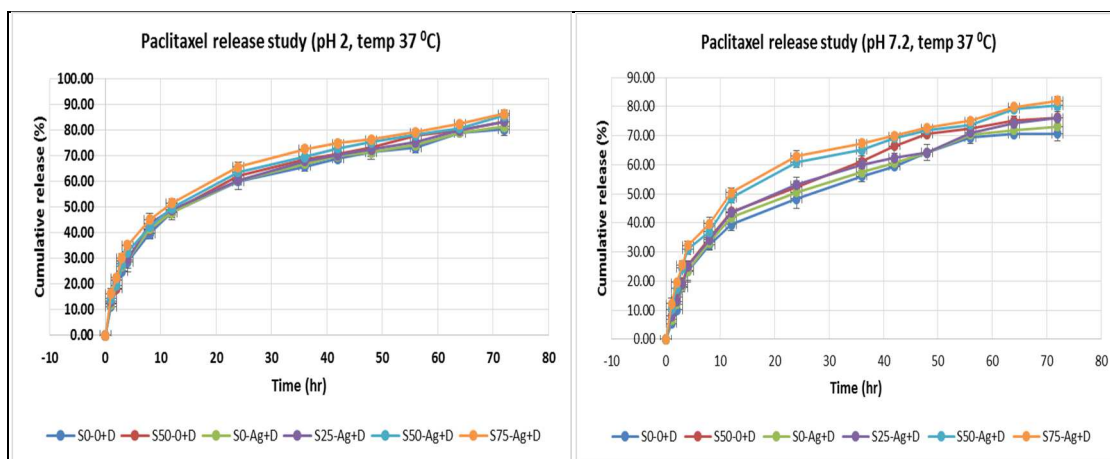
Fig. 2: *In vitro* release of drug paclitaxel from SA-g-Poly (acryl amide-co-acryl acid) cloisite-30B)/AgNPs hydrogel composites, the results were expressed as the mean of three observation, mean±SD (n =3)

The paclitaxel dissolution test of SA-PAAm-PAAc/C30B/AgNPs hydrogel composites were performed in dissolution device (LABINDIA DS8000) with the aid of the paddle technique laid out in USP XXIII. SA-PAAm-PAAc/C30B/AgNPs hydrogel composites were immersed in the 500 ml of dissolution medium (SGF). The content material became centrifuged at 100 rpm at 37 °C±0.5 °C ideal sink conditions were maintained in the paclitaxel dissolution study period. The stimulation of gastrointestinal transit condition was achieved by means of changing the pH of dissolution medium at different time periods. Paclitaxel release kinetics was analyzed with the aid of the following equation (Eqn.6), plotting the cumulative release profile versus time.

$$Equation\ Mt/M\infty = kt^n \dots\dots\dots\dots (6)$$

wherein Mt and $M\infty$ are the quantity of drug released via the hydrogel at time t and at equilibrium, k is a specific constant of the hydrogel, and n is a specific exponent of the mode of transport of the penetrate, the drug release from SA-PAAm-PAAc/C30B/Ag NPs hydrogel composites were studied in buffer medium of pH 2 and 7.2. The samples have been withdrawn from the dissolution medium at different time intervals using pipette fitted with a microfilter and the concentration of PT was measured by uv-spectrophotometer (LAB INDIA, UV-3092) at constant λ max. = 230 nm. The receptor volume was maintained constant changing the equivalent amount of stimulated gastro-intestinal fluids (SGF). The concentration of paclitaxel inside the samples was calculated primarily based on average calibration curves. All the dissolution studies were carried out in triplicate.

In order to determine the potential applications of SA-PAAm-PAAc/C30B/AgNPs based superabsorbent hydrogel composites containing a pharmaceutically active compound (PT), we've got investigated the drug paclitaxel release behaviour form this system under physiological conditions. The percentage of the released drug from the polymeric carriers as a characteristic of time t [19]. The concentration of paclitaxel delivered at selected time durations was determined by using the standard procedure. The % of drug release was plotted against time t and the cumulative release was calculated. As can be seen from the graphs when pH of the medium was 7.2, the cumulative release rate of paclitaxel from the test hydrogels is increased with increase in clay (C30B) content, in addition to the presence of AgNps. Also, the slightly fast and higher release rate of the drug in the case of $S_{75-Ag+D}$,(80±9 % within 72 h) in which clay content is 75 wt%. This difference in their swelling behaviour was responsible for the variation of the drug release rate [16, 18]. Indeed; the drug inside the hydrogel will be released as a result of the hydrogel composite volume change and interaction between the polymer network and the drug. The fractional release of the drug is at once proportional to the swelling ratio of the hydrogels. This result suggests that the better swelling ratios of the hydrogel create larger surface regions to diffuse the drug. And this follows the Nonfickian (Anomalous) type of diffusion mechanism. However, it is worth to mention that the release mechanism of a drug would depend on the selected dosage form, pH, nature of the drug, fillers, and polymer used [20].

Further, the *in vitro* release of PT drug from a biodegradable hydrogel nanocomposite systems are affected by the characteristics of the polymer, cloisite-30B and silver nanoparticles. Controlling the release is too controlling the properties affecting release, consisting of particle size, size distribution, drug content, properties of polymer and surface properties [21].

FT-IR analysis

The FT-IR spectrum of synthesized SA -PAAm-PAAc/C30B/AgNPs hydrogel composites were evaluated, results show that the synthesized hydrogel composites displayed good compatibility between SA-PAAm-PAAc polymers with significant changes after incorporation of cloisite-30B and silver nanoparticles into hydrogel network and the corresponding IR peaks as shown in fig. 3.
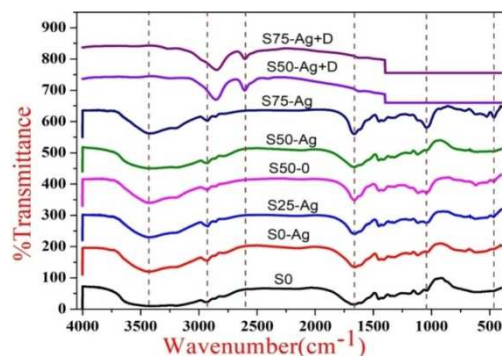

Fig. 3: FT-IR Spectrum of SAPAAmPAAc/C30B/AgNPs hydrogel composites

A peak appeared at 3400 cm^{-1} indicating the presence of hydrogen bonding between SA and PAAm-PAAc polymers causing OH/NH$_2$ stretching [4] 3400 cm^{-1} in SA-g-PAAm-PAAc and drug-loaded one corresponds to the presence of–O-H stretching vibrations of hydroxyl group in the SA backbone, more broadening of 3400 cm^{-1} stretch truly suggests that intermolecular hydrogen bond formation within the SA-g-PAAm-PAAc and drug-loaded SA-g-PAAm-PAAc hydrogel composite samples.

For all samples the absorption peaks of strong broad band intensities in the range between the 3349.18 to 3427 cm^{-1}indicates the O-H stretch (hydrogen bonded) and the peaks in the range, for all samples were at 2920.45 cm^{-1} to 2932.23 cm^{-1} shows the strong C-H stretching frequencies, further the stretching frequencies for all the samples except S $_{50-Ag}$ in the range between 1658.86 cm^{-1} to 1667.49 cm^{-1}, represents C=C variable stretching frequencies, whereas the sample S$_{50-Ag}$ shows stretching variable frequencies at

higher wavenumber values of 2104.53 cm^{-1}for–C=C-bonds of SA and PAAm-PAAc interaction.

Typically, Hydrogen bond took place among proton donor and proton acceptor atoms. The lone pair of electrons–O-of PAAm-PAAC should interact with–H atoms of SA and formed intermolecular asymmetrical stretching vibrations at 1600 cm^{-1} in SA showed the presence of–COO group. The characteristic peak at 1600-1668 cm^{-1} in all the samples was due to amide groups (-CONH2) of PA (>C=O stretch) [22] the bands at 2900-2950 cm^{-1} had been because of–C-H stretch of–CH2 groups of PAAm and PAAc polymers.

Conversion of 1094 and 1030 cm^{-1} stretching band of SA (1012,1044,1114,1042,1020, 1045 cm^{-1}) in to singlet,1041 cm^{-1}absorption stretch in SA-PAAm-PAAc denotes the formation of secondary alcohol (characteristic peak of–CH-OH in cyclic alcohol C-O stretch) during the course of grafting,this shift in the direction of lower frequency shows weakening of–C-C-and–C-O-bonds [23,24]. Stretching vibration at 1456 cm^{-1} for the C-N group can be observed within the FT-IR spectrum of drug loaded and non-drug loaded SA-PAAm-PAAc hydrogel composites, which did not see in the spectrum of pure SA [25]. The intermolecular hydrogen bond provides an extra mechanical strength to the grafted polymer, those differences supported the successful grafting of acrylamide and acrylic acid on SA.

The intensity peaks in the range between all the samples except S$_{50-Ag}$ are 1406.55 cm^{-1} to 1455.13 cm^{-1} which indicates–C-H variable bending frequencies may be due to the presence of acid groups in SA and PAAm-PPAc interactions and modifiers used during the modification of cloisite-30B clay. But the sample S$_{50-Ag}$ showing the frequency vibrations at 1667.02 cm^{-1} this is an extraordinary behavior of the sample S$_{50-Ag,}$ Again all the samples except S$_{50-Ag}$ and S$_{50-AgD}$ (drug loaded) samples exhibits strong stretching frequencies in the range of 1011.94 cm^{-1} to 1118.84 cm^{-1} may be due to the presence of C-O or C-F groups in ethers or in esters two bands or more, and also in the frequency range of 1315.57 cm^{-1} to 1323 cm^{-1} except for the samples S$_{50-Ag}$, S$_{50-AgD}$ (drug loaded) and S$_{75-Ag}$ may be due the C-O stretching of acid group present in SA and also may be due to C-O in ester group. Further, in the frequency range between 951 cm^{-1} to 1045 cm^{-1}attributes C-O stretching except at 951 cm^{-1} frequency for =C-H bending vibrations.

In trendy, there has been no sizable modifications of functional groups discovered in all the nanocomposite hydrogels which includes the nanofillers (AgNPs and clay mineral-C30B), which shows that the structure of the SA-PAAm-PAAc hydrogel composites have not been changed inside the carbohydrate region (700–1700 cm^{-1}) by mixing with the nanoparticles (AgNPS). But, the intensity of the peaks increased in all the SA-PAAm-PAAc/C30B/AgNPs composite hydrogels that are presumably because of the Vander Waals forces among AgNPs and the SA-PAAm-PAAc polymers [26]. Consequently, there has been no change in the intensity of peaks of clay mineral present in the composites, which may be because of the formation of weak intermolecular hydrogen bond among SA-PAAm-PAAc hydrogels and clay mineral particles. Comparable patterns of FT-IR spectroscopic results were found in the nanocomposite hydrogels with combined use of AgNPs and clay mineral-C30B. Such increase in strength of nanocomposite hydrogels has been frequently found with other biopolymer-based nanocomposites such as agar/clay mineral [27] and agar/AgNPs nanocomposite films [28].

Thermogravimetric analysis

Thermogravimetric analysis (TGA) and differential scanning calorimetric analysis (DSC)were carried out within the range of 30-800 °C at the heating rate of 20 °C/min. in presence of N$_2$ (100 ml/min.) and the graphs have been plotted weight % and heat flow respectively versus temperature in °C as shown in fig. 4, 5, 6.

The sample, S$_{0-0}$, exhibits glass transition temperature (Tg) at 75 °C. This formulation does not contain cloisite-30B and silver nanoparticles. Therefore it is just like, the plain sample of sodium alginate–polyacrylamide-poly acrylic acid (SA-PAAm-PAAc) hydrogel. The sample S$_{0-Ag}$, is the sample without clay and with silver nanoparticles, similar Tg was observed, as which shown in the case of formulation S$_{0-0}$, so the presence of silver nanoparticles do not influence the thermal stability of the sample, but major thermal decomposition was observed in the formulations S$_{0-0}$, S$_{50-0}$ S$_{50-Ag}$ and S$_{75-Ag}$ in the range of 280-300 °C except in the case of S$_{25-Ag}$, this may be caused due to clay-silver nanoparticle composition in the sample, that is 25 wt% of cloisite-30B with AgNps may be the best composition to show better thermal stability when compared to other samples.

Fig. 4, 5, 6 shows, the formulations S$_{0-0}$ and S$_{0-Ag}$ exhibit 4 exothermic peaks and 3 endothermic peaks, endotherms may be due to the reason that, absorption of moisture by the samples, whereas S$_{25-Ag}$ and S$_{50-0}$ show 3 exothermic peaks and 3 endothermic peaks. S$_{50-Ag}$ and S$_{75-Ag}$ show 2 exothermic and 2 endothermic peaks. Among all exothermic peaks, major thermal decomposition was observed at the temperature range of 270 °C-300 °C. Before that temperature range, they exhibit thermal stability and all the samples show endothermic peaks at 380 °C-450 °C temperature range.
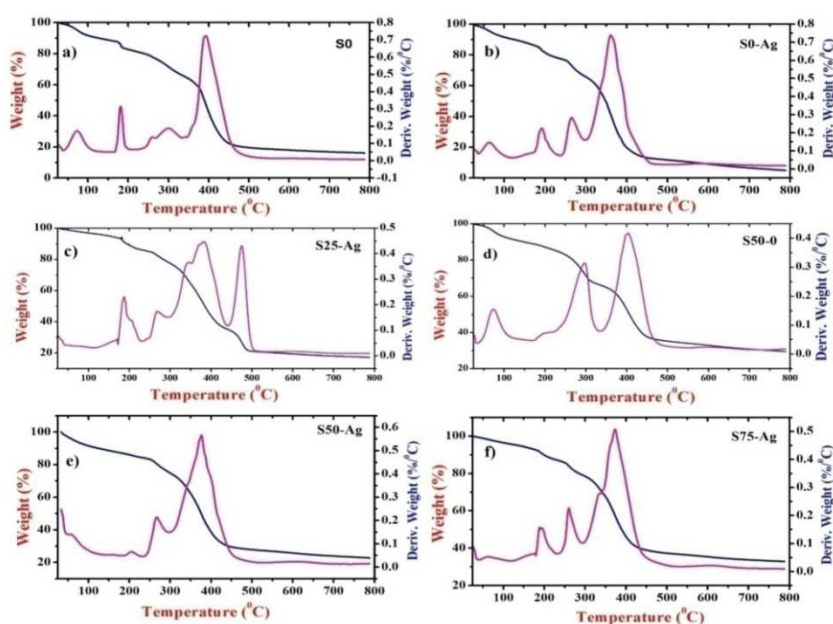
TG-DSC studies

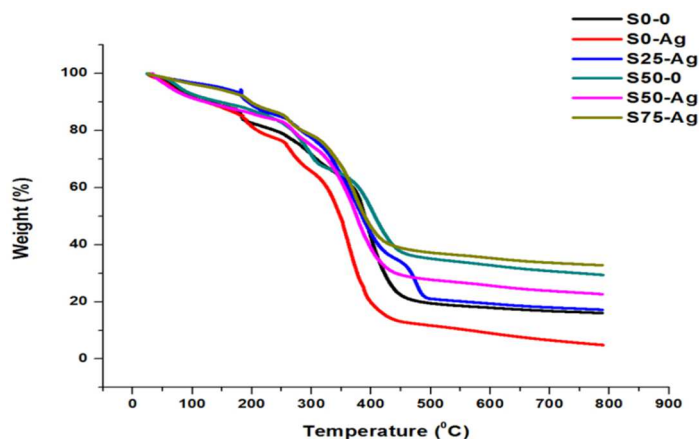**Fig. 4: TGA and DSC of SA-PAAm-PAAc/C30B/AgNPs hydrogel composites**

Fig. 5: TGA of SA-PAAm-PAAc/C30B/AgNPs hydrogel composites

DSC for all the samples S_{0-0}, S_{25-Ag}, S_{50-0}, S_{50-Ag} and S_{75-Ag} which are shown in fig. 4, 5, 6 which indicates, except S_{0-0} and S_{50-0} samples the Tg was slightly decreased because of absence of cloisite-30B, but in the presence of clay and AgNps in the samples attributes to decrease in the cross-linking density, thus decreases the thermal stability. Actually, the presence of clay should increase the Tg. In DSC graph it has been observed that the appearance of sharp peaks at the temperature range of 280 °C-310 °C may be due to the polymorphism and melt, however in the case of S_{50-0}, S_{50-Ag} and S_{75-Ag} no such thermal degradation was observed at 390-410 °C, whereas, for S_{0-0}, S_{0-Ag} and S_{25-Ag} further mild prevalence of degradation was found. In trendy TGA offers data on the thermal stability of the hybrid nanocomposites with reference to polymers which include SA (sodium alginate), PAAm and PAAc. In the fig. 4, 5, 6. It has been observed that all samples of hybrid hydrogel nanocomposites have 4 different decomposition steps and 95% thermal degradation of hydrogel chains took place at 800 °C, however, it is cited as four degradation steps (multi-step degradation). the first major step starts around 150 °C which suggests that weight reduction due to the evaporation of water molecules and second predominant step starts from 350 °C with 90% weight loss were occurred even at 500 °C for all the samples, except S0-Ag and (two minor steps, negligible weight loss especially in plain/virgin hydrogels) (S0-0) formulations.

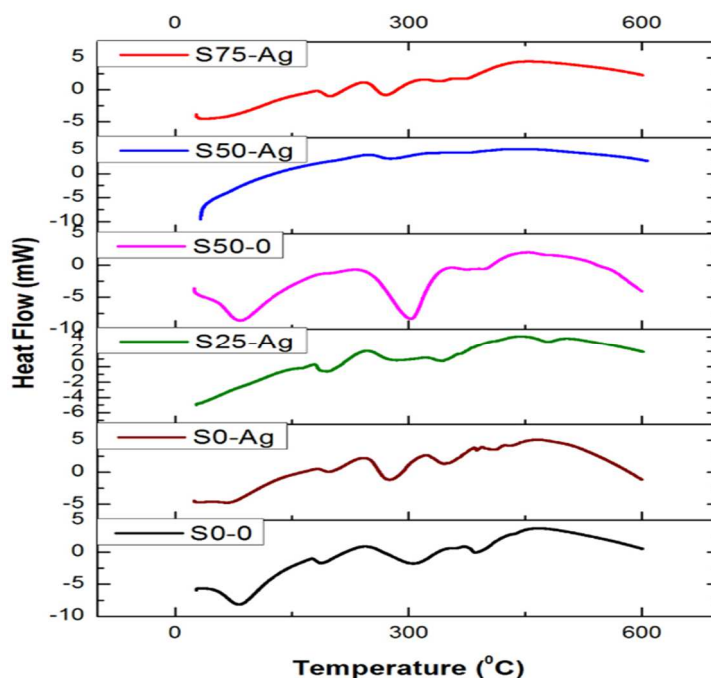**Fig. 6: DSC of SA-PAAm-PAAc/C30B/AgNPs hydrogel composites**

In the case of S_{0-Ag}, 90% of weight loss was observed below 370 °C. The difference in decomposition between the pure hydrogel and S_{0-Ag} and cloisite-30B/AgNPs nanocomposite hydrogels are found in between 20-25% and it confirms that the presence of AgNPs and cloisite-30B clay in the hydrogels, as the percentage of clay (cloisite-30B), increases along with the presence of AgNps which increases the difference in weight loss and it will likely to be in very large. In present study cloisite-30B and AgNPs in aggregate play a major role, in the decrease of thermal degradation of hydrogel composites and also which reduces the % of weight loss [29]. The difference in weight loss, in comparison to the formulation S_{0-0}, has larger difference in wt. loss and lesser will be the thermal stability of the sample, further S_{75-Ag} has a larger difference of wt. loss (33%) when compared to S_{0-0} formulation (larger the difference, more stable will be the sample) S_{75-Ag} has the difference of wt. loss with respect to S_{0-0} is 27.5 %, S_{50-Ag}-24.16%, S_{50-0}-23.57 %, S_{25-Ag}-12.23% and S_{0-Ag}-

10.95%. This data indicates that the formulation S_{75-Ag} is more thermally stable compared to all other samples and S_{0-Ag} is least thermally stable when compared to the rest, lower the difference, lesser will be the thermal stability and larger the difference (in terms of wt. loss), higher will be the thermal stability of the formulations.

XRD analysis

X-ray spectroscopy of various formulations as shown in the fig. 7. XRD analysis of SA-PAAm- PAAc/C30B/AgNPs hydrogel composites indicate the decrease in crystallinity of pure SA was because of formation of new polymer system (SA-PAAm-PAAc)
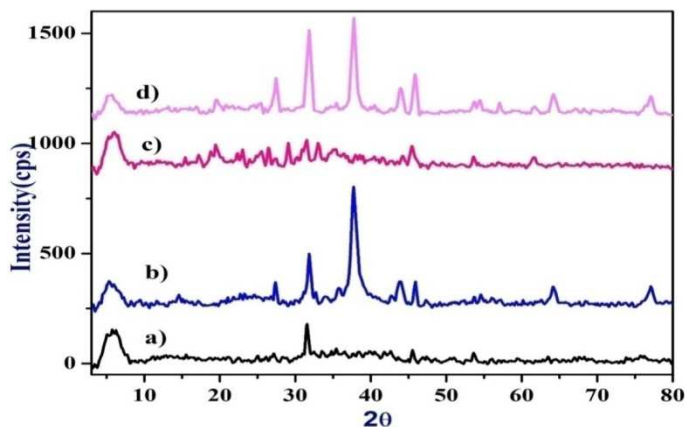

Fig. 7: XRD of SA-PAAm-PAAc/C30B/AgNPs hydrogel composites. XRD lines a), b), c),d) indicates intensity peaks for the formulations S_{0-0}, S_{0-Ag}, S_{50-0} and S_{50-Ag} respectively

XRD of SA exhibiting characteristic peaks at 19 °, 28 °, 28.9 °, 32.5 ° and 33.5 ° 2θ, while in the case of SA-PAAm-PAAc hydrogels no such sharp peaks had been observed, suggesting the complete transformation of SA into SA-PAAm-PAAc new polymer hydrogels. The FTIR spectrum additionally supported the grafting of PAAm and PAAc on to SA and within the drug-loaded gels, Addition of extra bulky groups, i.e. polyacrylamide (PAAm) and polyacrylic acid (PAAc) on to the backbone of SA may reduce the overall crystallinity and also decrease the intermolecular hydrogen bond [26].5 ° and 19.79 ° of cloisite-30B corresponding to planes (001) and (020) respectively, confirming the predominance of cloisite-30B in the samples. This suggests that increased interlayer spacing (basal) of organic-clays based on the way in which it is guided between the lamellae of clay minerals [30].

Anticancer study

The cytotoxicity of extracts from hydrogel composites on HaCaT cells was determined by the MTT assay [31]. In the present investigation, the cytocompatibility of the obtained hydrogel composites was examined in regular epithelial HaCaT cellular strains. Fig. 8, 9 depicts the relative proliferation rate of the two

cellular lines while assessed through MTT assay. NAD (P) H-dependent cell oxidoreductase enzyme inside the mitochondria has the capability to reduce the MTT dye (3-(4, 5-dimethylthiazol-2-yl)-2, 5-diphenyl tetrazolium bromide) to insoluble formazan [32].

The formation of formazan depends upon the rate of cellular metabolism, so the cells treated with the different leachant percentage should theoretically have the normal rate of metabolism. This indicates that the gels had been cytocompatible in nature. No visual difference became located inside the cellular morphology, suggesting the absence of the unfavorable impact of the leachants on mobile proliferation.

As a substitute, the prepared formulations supported the growth of HaCaT cell line to a certain level in comparison to the control. Again the cell viability decreases with the increase in clay % as well as in the presence of Ag nanoparticles in the gel composites, especially the formulations $S_{50-Ag+D}$, $S_{75-Ag+D}$ show better anticancer activity than rest of others (in MCF-7 cell lines). Finally, the biosynthesized AgNPs of C30B clay based hydrogel composites shows significant anticancer activity, and thus, it can be used as a potential source for various biomedical applications [33].
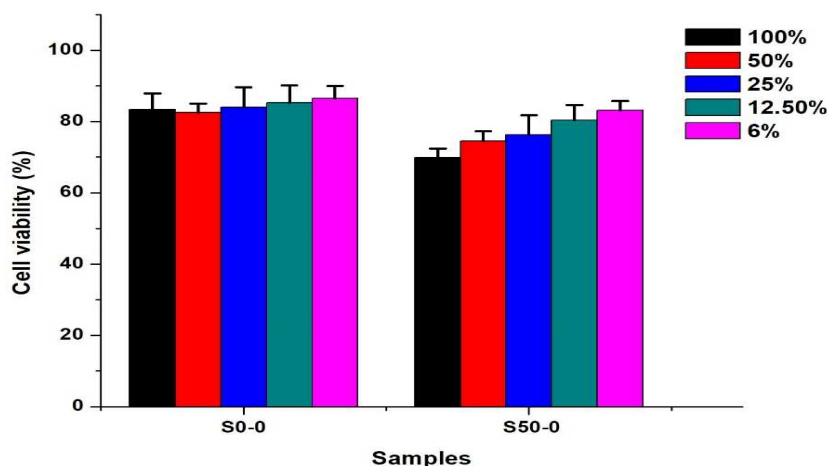

Fig. 8: Cell viability of S_{0-0}, S_{50-0}. The MTT assay was used to measure the viability of HaCaT cells at various dilute extract solution concentrations. Media at 100% was used as a control. The results were expressed as the mean of three observation, mean±SD (n =3)
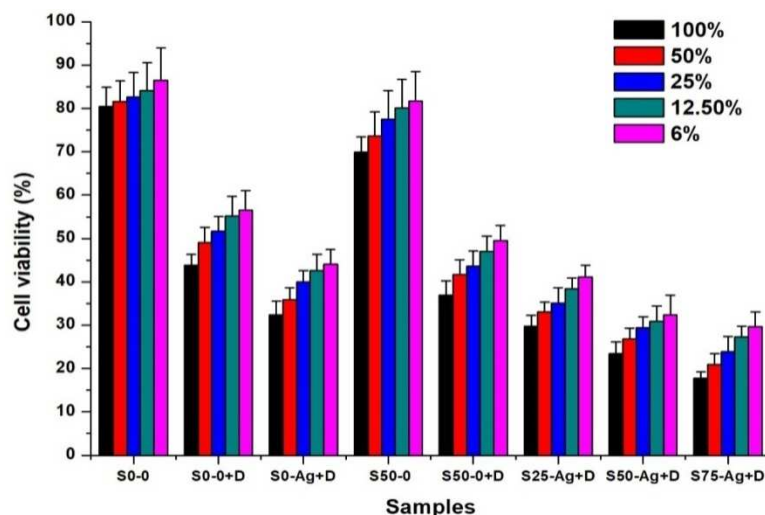
Fig. 9: Cell viability of S$_{0-0}$, S$_{50-0}$, S$_{0-0+D}$, S$_{50-0+D}$, S$_{0-Ag+D}$, S$_{25-Ag+D}$, S$_{50-Ag+D}$, S$_{75-Ag+D}$. The MTT assay was used to measure the viability of MCF-7 cells at various dilute extract solution concentrations. Media at 100% was used as a control. The results were expressed as the mean of three observations, mean±SD (n =3)

CONCLUSION

Hydrogel composites of sodium alginate grafted PAAm-PAAc/ C30B/Ag was prepared by free radical polymerization method and AgNPs have been successfully incorporated into them by chemical reduction method and used to produce sustained delivery of paclitaxel for the treatment of cancer. *In vitro* release studies suggest that co-grafting of SA with PAAm-PAAc/C30B/AgNPs could be a useful tool for the sustaining the delivery of drugs within the stomach. Swelling, FT-IR, XRD analysis, and DSC--TGA has suggested the successful grafting (basically attachment of amide bond of polyacrylamide with the carboxyl group of SA) of PAAmPAAc. DSC and XRD data reveal the dispersion and amorphization of crystalline Ag, drug, and C30B within the matrix of SA-PAAm-PAAc/C30B/AgNPs hydrogel composites. The samples S$_{75-Ag}$, S$_{50-Ag}$ exhibits profound swelling capacity than the rest of the other samples due to the simultaneous presence of C30B and AgNPs with the increase in % wt of C30B in the respective samples. *In vitro* drug release confirmed the release up to 72 h at the rate of 80±9 %, whereas gels were able to float up to 85 h. The increase of the percentage of grafting, as well as decrease in the amount of C30B, could reduce the release rate of the drug; however, it increases the drug loading within the SA-g-PAAm-PAAc grafted gastro-retentive polymer composite hydrogels. The swelling of grafted SA-g-PAAm-PAAchydrogel network is strongly interdependent on the cross-linking and polymerization process. The drug release depends upon the extent of gelation which was based on cross-linking and amount of graft copolymer used. This study could prove to be a platform to explore the possibility of grafting technology for the preparation of gastro retentive hydrogel-based drug delivery systems. The formulations S$_{75-Ag}$, S$_{50-Ag}$, andS$_{25-Ag}$ shows better anticancer activity and slightly higher rate of sustained drug delivery than the rest of other (samples without AgNPs and C30B)

AUTHORS CONTRIBUTIONS

All the authors have contributed equally

CONFLICT OF INTERESTS

The authors declare no conflict of interests

REFERENCES

1. Kulkarni PV, Keshavayya J. Preparation, and evaluation of polyvinyl alcohol transdermal membranes of salbutamol sulfate. Int J Curr Pharm Res 2010;2:29-32.
2. Khurana IS, Kaur S, Kaur H, Khurana RK. The multifaceted role of clay minerals in pharmaceuticals. Futuristic OA 2015;1:FS06.
3. Parida UK. Synthesis and characterization of chitosan-polyvinyl alcohol blended with cloisite 30B for controlled release of the anticancer drug curcumin. J Biomater Nanobiotechnol 2011;2:414–25.
4. Vimala K, Yallapu MM, Varaprasad K, Reddy NN, Ravindra S, Naidu NS, *et al*. Fabrication of curcumin encapsulated chitosan-PVA silver nanocomposite films for improved antimicrobial activity. J Biomater Nanobiotechnol 2011;2:55–64.
5. Thoniyot P, Tan MJ, Karim AA, Young DJ, Loh XJ. Nanoparticle–hydrogel composites. Concept, design, and applications of these promising, multi-functional materials. Adv Sci 2015;2:1–13.
6. Remunan-Lopez C, Bodmeier R. Mechanical, water uptake and permeability properties of cross-linked chitosan glutamate and alginate films. J Controlled Release 1997;44:215–25.
7. Pongjanyakul T. Alginate-magnesium aluminium silicate films: the importance of alginate blocks structures. Int J Pharm 2009;365:100–8.
8. Thomas V, Namdeo M, Mohan YM, Bajpai SK, Bajpai M. Review on polymer, hydrogel and microgel metal nanocomposites: a facile nanotechnological approach. J Macromol Sci Part A Pure Appl Chem 2008;45:107–19.
9. Asha Rani PV, Low KahMun G, Hande MP, Valiyaveettil S. Cytotoxicity and genotoxicity of silver nanoparticles in human cells. ACS Nano 2009;3:279–90.
10. Jain J, Arora S, Rajwade JM, Omray P, Khandelwal S, Paknikar KM. Silver nanoparticles in therapeutics: development of an antimicrobial gel formulation for topical use. Mol Pharm 2009;6:1388–401.
11. El-Ansari A, Al-Daihan S. On the toxicity of therapeutically used nanoparticles: an overview. J Toxicol 2009:1–9. http://dx.doi.org/10.1155/2009/754810
12. Zhang Z, Mei L, Feng SS. Paclitaxel drug delivery systems. Expert Opin Drug Delivery 2013;10:325–40.
13. Patil V, Belsare D. Development and evaluation of novel drug delivery system of tolterodine tartrate. Int J Appl Pharm 2017;9:186-93.
14. Hago EE, Li X. Interpenetrating polymer network hydrogels based on gelatin and PVA by biocompatible approaches:

synthesis and characterization. Adv Mater Sci Eng 2013:1-8. http://dx.doi.org/10.1155/2013/328763

15. Harshil P Shah, Shailesh T Prajapati, Patel CN. Gastroretentive drug delivery systems: from conception to commercial success. J Crit Rev 2017;4:1-21.

16. Bartil T, Bounekhel M, Cedric C, Jeerome R. Swelling behavior and release properties of pH-sensitive hydrogels based on methacrylic derivatives. Acta Pharm 2007;57:301–14.

17. Zhang J, Wang Q, Wang A. Synthesis and characterization of chitosan-g-poly(acrylic acid)/attapulgite superabsorbent composites. Carbohydr Polym 2007;68:367–74.

18. Hosseinzadeh H. Controlled release of a poorly water-soluble drug from amphiphilic and pH-sensitive chitosan-based hydrogel. Int J Pharma Bio Sci 2011;2:1–9.

19. Hoare TR, Kohane DS. Hydrogels in drug delivery: progress and challenges. Polymer 2008;49:1993–2007.

20. Nanjunda Reddy BH, Rauta PR, Venkatalakshimi V, Sreenivasa S. Synthesis and characterization of cloisite-30B clay dispersed poly (acrylamide/sodium alginate)/AgNp hydrogel composites for the study of BSA protein drug delivery and antibacterial activity. Mater Res Express 2018;5. https//doi.0rg/ 10.1088/2053-1591/aaac4c

21. Kohli S, Pal A, Jain S. Preparation, characterization, and evaluation of poly (lactide–co–glycolide) microspheres for the controlled release of zidovudine. Int J Pharm Pharm Sci 2017;9:70-7.

22. Soppimath KS, Aminabhavi TM, Kulkarni AR, Rudzinski WE. Biodegradable polymeric nanoparticles as drug delivery devices. J Controlled Release 2001;70:1–20.

23. Şolpan D, Torun M, Güven O. The usability of (sodium alginate/acrylamide) semi-interpenetrating polymer networks on the removal of some textile dyes. Appl Polym Sci 2008;108:3787–95.

24. Sutar PB, Mishra RK, Pal K, Banthia AK. Development of pH-sensitive polyacrylamide grafted pectin hydrogel for controlled drug delivery system. J Mater Sci Mater Med 2008;19:2247–53.

25. Shi XN, Wang WB, Wang AQ. Effect of surfactant on porosity and swelling behaviours of guar gum-g-poly(sodium acrylate-co-styrene)/attapulgite superabsorbent hydrogels. Colloids Surf B Biointerfaces 2011;88:279–86.

26. Shameli K, Ahmad MB, Yunus ZW, Ibrahim A, Jokar M, Darroudi M. Synthesis and characterization of silver/polylactide nanocomposites. World Acad Sci Eng Technol 2010;64:573–9.

27. Rhim JW, Lee SB, Hong SI. Preparation and characterization of agar/clay nanocomposite films: the effect of clay type. J Food Sci 2011;76:40–8.

28. Rhim JW, Wang LF, Hong SI. Preparation and characterization of agar/silver nanoparticles composite films with antimicrobial activity. Food Hydrocoll 2013;33:327–35.

29. Reddy PRS, Eswaramma S, Rao KSVK, Lee YI. Dual responsive pectin hydrogels and their silver nanocomposites: swelling studies, controlled drug delivery, and antimicrobial applications. Bull Korean Chem Soc 2014;35:2391–9.

30. Alhassan SM, Qutubuddin S, Schiraldi DA. Graphene arrested in the laponite-water colloidal glass. Langmuir 2012;28:4009–15.

31. Melanathuru V, Rangarajan S, Thangavel N. Comparative study of the antioxidant and anticancer activity of Alpiniacalcarata and Alpinia galangal. Int J Pharm Pharm Sci 2017;9:186-93.

32. Berridge MV, Herst PM, Tan AS. Tetrazolium dyes as tools in cell biology: New insights into their cellular reduction. Biotechnol Annu Rev 2005;11:127–52.

33. Lotha R, Subramanian AS, Muthuraman MS. Silver nanoparticles from medicinally important euphorbia cyathophora extract: biosynthesis, characterization, and anticancer activity. Asian J Pharm Clin Res 2018;11:154-6.